Mechanisms Determining the Atmospheric Response to Midlatitude SST Anomalies

SHILING PENG AND JEFFREY S. WHITAKER

NOAA–CIRES Climate Diagnostics Center, University of Colorado, Boulder, Colorado

(Manuscript received 3 February 1998, in final form 29 June 1998)

ABSTRACT

Previous GCM experiments demonstrated that a model atmosphere produces two different responses to a midlatitude warm SST anomaly over the Pacific under perpetual January and February conditions. To elucidate the mechanisms responsible for the different GCM responses and their dependence on the background flow, experiments with two idealized models are conducted. Experiments with a linear baroclinic model reveal that the GCM responses at equilibrium are primarily maintained by the anomalous eddy forcing. The anomalous flow induced directly by an idealized initial heat source exhibits little sensitivity to the background flow. Eddy feedbacks on the heating-induced anomalous flow are examined using a linear storm track model. The anomalous eddy forcing produced by the storm track model is sensitive to the basic state. The eddy forcing in January acts to shift the heating-induced upper-level ridge toward the northeast of the Gulf of Alaska, while in February it acts to reinforce the ridge. This suggests that the differences in the GCM responses are primarily associated with differences in the response of synoptic eddies to the presence of an anomalous ridge at the end of the Pacific storm track.

The idealized model experiments are also performed with the observed winter mean flow. The eddy feedbacks depend on the position of the heating relative to the storm track. With the heating centered over the western Pacific the eddy-driven anomalous flow reinforces the ridge over the Pacific, similar to that in GCM February, but much stronger. No such reinforcement by the transients is found with the heating shifted over the eastern Pacific. These results suggest that SST anomalies over the western Pacific perhaps play a more active role in midlatitude atmosphere–ocean interactions.

1. Introduction

Understanding the role of midlatitude sea surface temperature (SST) anomalies in climate variability on seasonal-to-decadal timescales remains a challenge. Midlatitude SST anomalies often persist for months and involve a low-frequency component on the decadal timescale (Deser and Blackmon 1995; Nakamura et al. 1997a). Observational analyses suggest that SST anomalies are initiated largely by atmospheric fluctuations, evidenced in stronger correlations as the atmosphere leads the ocean (Palmer and Sun 1985; Wallace and Jiang 1987; Deser and Timlin 1997). Whether SST anomalies also exert significant feedbacks on the atmosphere is as yet unclear. Since the atmosphere responds quickly to external forcing, oceanic feedbacks on the atmosphere can be immersed in nearly simultaneous relationships, not easily diagnosable by observational analyses. Therefore, causality has been sought through model simulations.

Model experiments with midlatitude SST anomalies so far have produced diverse results. The atmospheric responses to SST anomalies simulated by various general circulation models (GCMs) vary not only in magnitude but also in nature (Palmer and Sun 1985; Pitcher et al. 1988; Ting 1991; Kushnir and Lau 1992; Lau and Nath 1994; Ferranti et al. 1994; Latif and Barnett 1994; Kushnir and Held 1996). While a distinction may be drawn between the results of high- and low-resolution models as discussed in Peng et al. (1997), noticeable differences also exist among the results of comparable high-resolution GCMs. To isolate the causes for these discrepancies idealized GCM experiments were conducted by Peng et al. (1995) with an identical Atlantic SST anomaly but two different model states. The model responses to the SST anomaly in early winter (November) and midwinter (January) were found to be drastically different. Using a similar approach, GCM experiments were conducted with a Pacific SST anomaly by Peng et al. (1997). Their results confirm that the atmospheric response to a midlatitude anomaly strongly depends on the GCM climatology. Critical changes in the climatology, due to either natural seasonal shifts (Peng and Fyfe 1996) or unrealistic model behaviors, can significantly affect the nature and intensity of the response.

The GCM experiments of Peng et al. (1997, hereafter

Corresponding author address: Dr. Shiling Peng, NOAA–CIRES/CDC, R/E/CD1, 325 Broadway, Boulder, CO 80303-3328.
E-mail: sp@cdc.noaa.gov

PRH) showed that with an identical warm SST anomaly the model atmosphere produces a baroclinic response in perpetual January but a nearly equivalent barotropic ridge in February. Diagnoses of the thermodynamic budget suggest that the different responses are probably related to the difference in the background meridional flow. The background flow difference between January and February is unrealistically amplified in the model. By comparison, the simulated background flow in February is more realistic, suggesting that the February response to the SST anomaly may also be more representative of nature. Clearly, a realistic assessment of the effects of midlatitude SST anomalies on the atmosphere depends on the GCM's fidelity in describing observed climatology.

Identifying those aspects of the model climatology that led to the differences in the January and February responses is a challenging task. The budget analysis of PRH indicates that the strength of the background meridional flow may have played a role in determining the responses. Such a diagnosis of the equilibrium balances cannot establish causality. It remains unclear by what mechanisms the different responses are induced. Mean flow differences over the midlatitude oceans are always related to the difference in high-frequency transients, reinforcing each other at equilibrium (Branstator 1992, 1995). The responses may also be affected by other factors, such as the strength and structure of the diabatic heating. A better understanding of the problem is sought in this study through systematic experiments with the idealized models.

Two idealized models are adapted: a linear baroclinic model and a linear storm track model. Experiments are conducted in three steps. First, the baroclinic model is used to determine the maintenance of the GCM responses. Second, the baroclinic model is used to examine the atmospheric response to an idealized initial heating in the absence of eddy feedbacks. Third, the storm track model is employed to simulate the eddy feedbacks on the heating-induced anomalous flow, and their sensitivity to the basic state. Idealized model experiments are also conducted with observed winter flow to determine the eddy feedbacks in nature and their dependence on the heating position relative to the jet. Results of this study provide not only an explanation for the GCM responses of PRH but also valuable insights into midlatitude atmosphere–ocean interactions in nature.

The paper is organized with six sections. Section 2 describes the model configurations and the experimental approach. Section 3 examines the maintenance of the GCM responses. Section 4 discusses the role of the diabatic heating, and section 5 the eddy feedbacks. Summary and discussions are included in section 6.

2. Description of the models

Two idealized models are used in the following study: a linear baroclinic model (LBM) and a linear storm track model (STM). The model configurations and the experimental approach are described below.

a. Linear baroclinic model

The LBM is a time-dependent model based on the primitive equations. The model consists of five basic equations describing, respectively, the vorticity, divergence, temperature, mass, and hydrostatic balances. It is a global spectral model with a T21 spherical harmonic horizontal resolution and 10 equally spaced pressure levels. No topography is prescribed at the lower boundary. The model is linearized about a three-dimensional time-mean basic state and treats the diabatic heating and nonlinear eddy terms as forcing. Fluxes associated with nonlinear stationary terms are also treated as forcing, referred to as stationary nonlinearity following Branstator (1992). Perturbations from the basic state are interpreted as the linear model response to the forcing. Models as such are often used as a diagnostic tool to determine the dynamic maintenance of an anomalous flow by various forcing terms (Branstator 1992; Ting and Lau 1993; Ting and Peng 1995). A detailed description of the linearization procedure can be found in Branstator (1992).

Rather than attempting to invert the linear operator of the model, as in Ting and Lau (1993), we integrate the LBM forward in time until a steady state is reached. Rayleigh friction and Newtonian damping are given the rate of $(1\ \text{day})^{-1}$ at the lowest level, decreasing linearly to zero at 700 mb. A biharmonic diffusion with a coefficient of $2 \times 10^{16}\ \text{m}^4\ \text{s}^{-1}$ is applied in the vorticity, divergence, and thermodynamic equations. These levels of dissipation are sufficient to stabilize the model so that a steady state can be reached. As discussed by Ting and Lau (1993), eddy heat fluxes generally act to reduce the local temperature gradient. The thermal effects of the transients can be parameterized as an additional diffusion in the model. The validity of this paramerization has been verified with our GCM data. A thermal diffusion with a coefficient of $2 \times 10^6\ \text{m}^2\ \text{s}^{-1}$ is added to represent the eddy effects. A quasi-steady state is generally achieved after about 15 days, so for all the results presented below, we approximate the steady solution as the last 5-day average of a 20-day integration.

b. Linear storm track model

The STM developed by Whitaker and Sardeshmukh (1998, hereafter WS) is used to determine the synoptic eddy statistics associated with a given mean flow. It is a quasigeostrophic model linearized about a time-mean flow and forced with Gaussian white noise. With such a system the eddy covariance is linked to the spatial structure of the background flow by a fluctuation dissipation relation. This relation balances the general decaying tendency of the eddies with stochastic forcing and energetic interactions with the background flow to

achieve a statistically stationary state. The eddy statistics can thus be determined solely from the basic state (see WS for detailed procedure). As shown in WS, the spatial distributions of the eddy statistics produced by the STM for the observed winter flow compare favorably with observations. The model is also sensitive enough to basic state changes to produce reasonable variations in eddy statistics.

An updated STM, with a T31 horizontal resolution and five equally spaced pressure levels, is used in this study. For computational efficiency, hemispheric symmetry is imposed (as in WS). The static stability parameter is set to a constant for each layer. The corresponding potential temperature difference is determined by averaging observed winter temperature over the latitudinal band of 30°–60°N. Both Rayleigh friction and Newtonian damping are assigned timescales of 1.5 days at the lowest level and 15 days above. The coefficient of the biharmonic diffusion is set to 2×10^{16} m^4 s^{-1}. As in WS, a scaling constant is chosen so that the simulated 300-mb eddy kinetic energy for observed basic state matches observations. The STM, combined with the LBM, provides an effective tool for the study of feedbacks between synoptic eddies and low-frequency anomalies.

Our strategy is to determine first the maintenance of the GCM responses to the SST anomaly obtained by PRH. Eddy momentum fluxes and the diabatic heating from the GCM runs are used to force the LBM. These results determine the relative importance of each forcing in maintaining the equilibrium balance. The LBM is further used to examine the model response to an idealized initial heating without feedback from the transients, and its dependence on the heating structure and the background flow. Eddy feedbacks on the heating-induced anomalous flow, and their sensitivity to the basic state, are simulated using the STM. The anomalous eddy fluxes produced by the STM in turn are used to drive the LBM. In this way, the nature of the eddy feedbacks and their role in modulating the development of the GCM responses are determined.

3. Maintenance of the GCM responses

The GCM experiments of PRH were conducted to examine the atmospheric response to a midlatitude SST anomaly and its dependence on the model background state, using the National Centers for Environmental Prediction's MRF9 with a T40 horizontal resolution and 18 vertical levels. The experiments are performed for two model states: perpetual January and February. For each model state, four pairs of 96-month integrations are made with or without the SST anomaly included at the boundary. More detailed descriptions of the model and the experiments are given in PRH.

The SST anomaly used in the GCM experiments is shown in Fig. 1. The ensemble-averaged model responses of geopotential height at 250 and 850 mb, and in a vertical cross section along 40°N, are shown in Fig. 2. Clearly, the height responses to the SST anomaly in January and February are very different. Over the Pacific the response in January is baroclinic with a trough decreasing with height, whereas in February the response is nearly equivalent barotropic with a ridge growing with height. An equivalent barotropic ridge also exists in January but over the northeast of the Gulf of Alaska instead of the Pacific. The warm SST-ridge type of response as produced by our GCM in February has appeared in several other relatively high-resolution GCMs (Palmer and Sun 1985; Ferranti et al. 1994; Latif and Barnett 1994; Peng et al. 1995). Such a response, if strong enough, can reverse the polarity of the anomalous surface heat fluxes at equilibrium so that they act to reinforce the SST anomalies locally and downstream, as shown in Latif and Barnett (1994) and Peng et al. (1995). Potentially, this can lead to a positive atmosphere–ocean feedback with profound influences on climate variability.

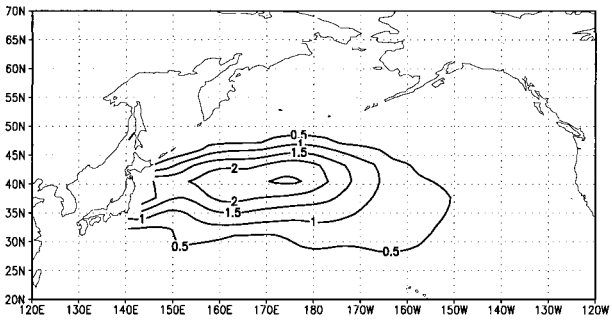

FIG. 1. The SST anomaly used in the GCM experiments. Contour interval is 0.5 K.

Since the model configuration, SST anomaly, and experimental design are identical in January and February, the different responses must have resulted from the difference in the model climatologies. The background flows averaged over the control runs, shown in Fig. 2 of PRH, illustrate that the jet is stronger and more tilted to the north at its exit in January than in February. Correspondingly, their Fig. 15 shows that the meridional flow east of the date line is nearly twice as strong in January as in February. In comparison with observations, the simulated background flow is more realistic in February, indicating that the February response to the SST anomaly may also be more realistic. Indeed, the warm SST-ridge type of response bears a qualitative resemblance to observed SST and geopotential height relations (Palmer and Sun 1985; Wallace and Jiang 1987). In order to understand by which mechanisms the different responses develop under the influence of different background flows, we examine first the maintenance of the GCM responses by various forcing terms. For this purpose, we rerun one pair of 96-month GCM experiments for both January and February to accumulate the submonthly transient fluxes and the diabatic

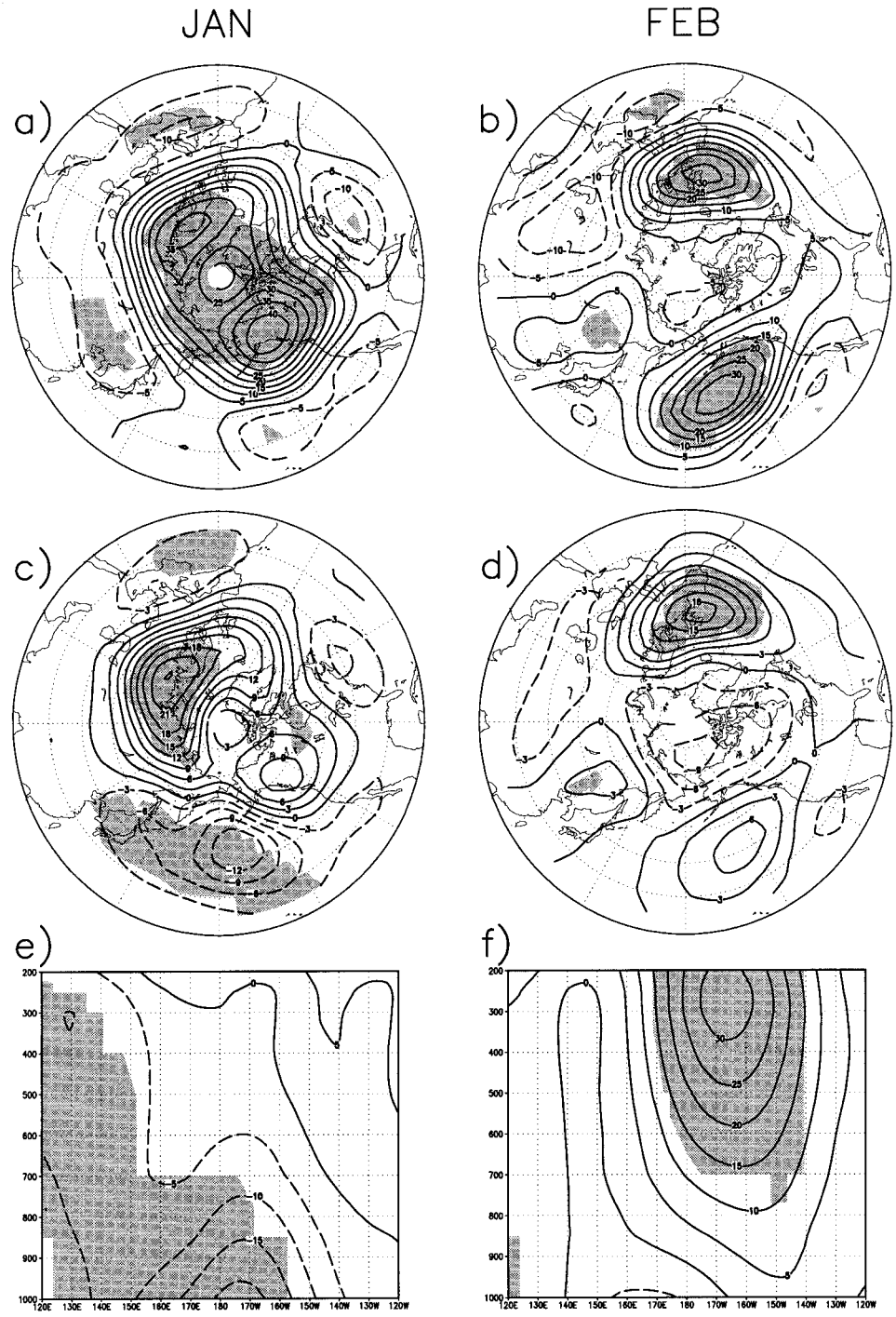

FIG. 2. The geopotential height response at 250 and 850 mb, and on a vertical cross section along 40°N (a), (c), and (e) for Jan and (b), (d), and (f) for Feb. Areas with the height anomalies significant at the 95% level are shaded. Contour interval for (a), (b), (e), and (f) is 5 m, and for (c) and (d) 3 m. In this and succeeding figures, dashed contours are used for negative values.

heating. The member chosen for the rerun in each month has a response most strongly resembling the ensemble mean response shown in Fig. 2. Since the February response is associated with a more realistic background flow, the following discussion will focus mainly on the February results. For brevity, the January results are described only for comparison.

The anomalous diabatic heating over the Pacific, av-

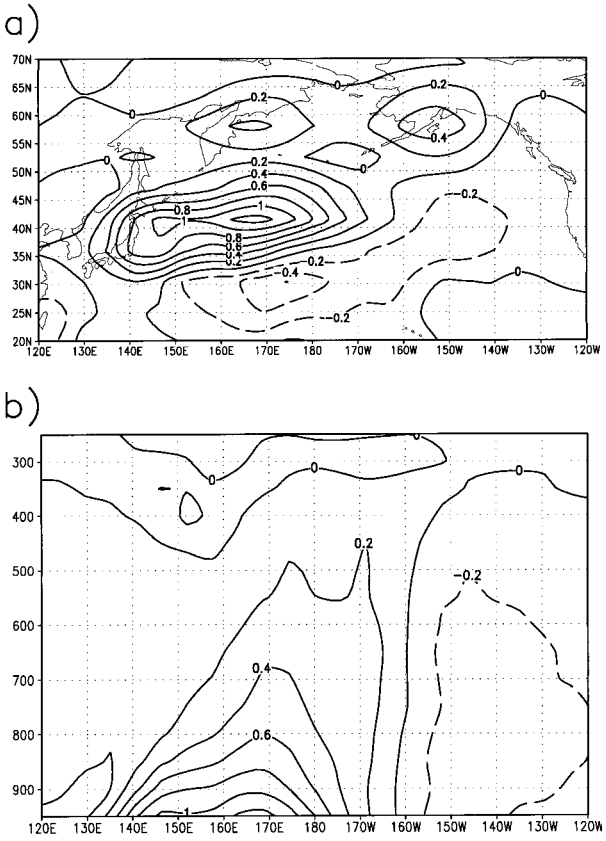

FIG. 3. The anomalous diabatic heating at (a) 950 mb, and (b) on a vertical cross section along 40°N, for Feb. Contour interval is 0.2 K day^{-1}.

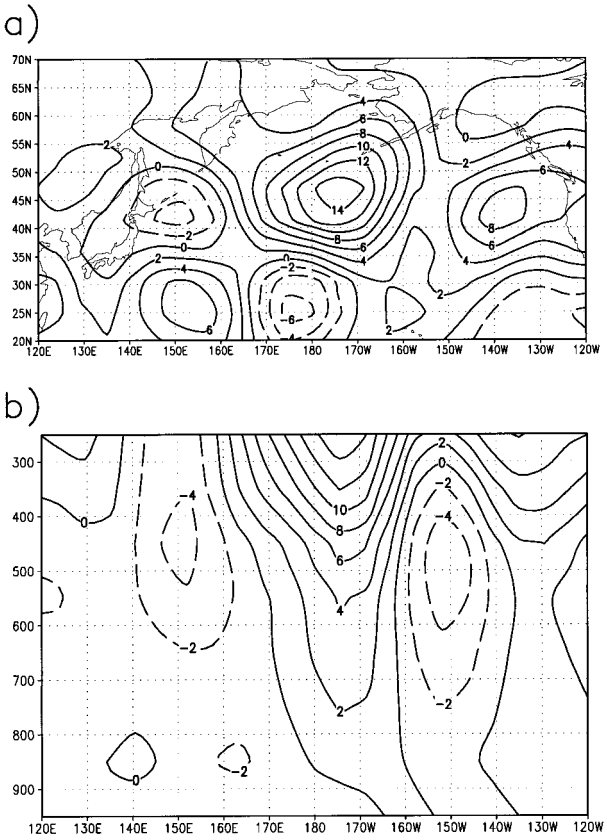

FIG. 4. Streamfunction tendency due to anomalous vorticity fluxes by submonthly transients at (a) 250 mb, and (b) on a vertical cross section along 45°N, for Feb. Contour interval is 2 m^2 s^{-2}.

eraged over the 96-month GCM rerun for February, is shown in Fig. 3a for 950 mb and Fig. 3b for a vertical cross section along 40°N. There is a positive heating center right above the SST anomaly at 950 mb and a weaker cooling to the southeast. The heating decreases and shifts slightly eastward with height. At equilibrium, the heating is very weak with a depth-averaged heating rate of less than 0.35 K day^{-1}. The anomalous streamfunction tendency due to vorticity fluxes by submonthly transients is shown in Fig. 4a for 250 mb and Fig. 4b for a vertical cross section dissecting the maximum along 45°N. The positive streamfunction tendency over the central Pacific indicates a reinforcement of the ridge response by the transients in February. The eddy forcing has a maximum of about 15 m^2 s^{-2} at 250 mb and a nearly equivalent barotropic structure. According to Ting and Lau (1993), the streamfunction tendency due to synoptic transients should be similar but weaker.

The above forcing from the GCM experiments is used to drive the linear model. The LBM response of geopotential height to the total forcing, including the diabatic heating, eddy vorticity fluxes, and stationary nonlinearity, is shown in Fig. 5. Clearly, the anomalous heights at 250 and 850 mb from the LBM (Figs. 5a,b) and those from the GCM (Figs. 2b, d) bear a strong resemblance. The LBM reproduces the large-scale features of the GCM response with some minor differences. For example, the anomalous ridge over the Pacific from the LBM is located about 5° north of that from the GCM. A vertical cross section dissecting the ridge maximum along 50°N drawn in Fig. 5c illustrates that the ridge has an equivalent barotropic structure, similar to that in the GCM. Given the different configurations of the two models, the similarity of the model results is very encouraging and demonstrates that the LBM is an effective diagnostic tool. One needs to keep in mind when making comparisons that only the forcing from one pair of GCM runs is used in the LBM.

The relative importance of the diabatic heating, eddy vorticity fluxes, and stationary nonlinearity in maintaining the anomalous flow shown in Fig. 5 is determined by running the LBM with each forcing, respectively. Both the diabatic heating and stationary nonlinearity are found to make minor contributions. Thus, the LBM response to the eddy vorticity fluxes shown in Fig. 6 is nearly identical to that shown in Fig. 5. The striking similarity between the responses demonstrates that the equilibrium anomaly in the GCM is primarily maintained by anomalous eddy vorticity fluxes, consistent with the results of Ting and Peng (1995). The LBM

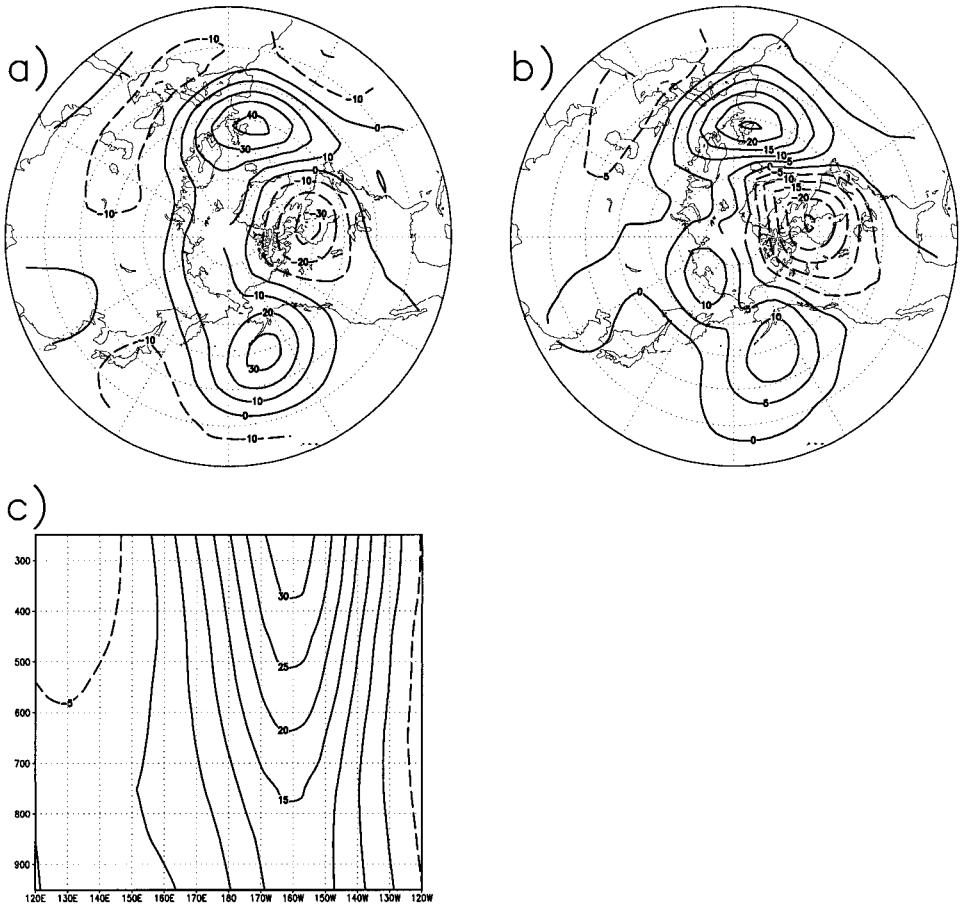

FIG. 5. The LBM geopotential height response at (a) 250 mb, (b) 850 mb, and (c) on a vertical cross section along 50°N, to the total anomalous forcing, including eddy vorticity fluxes, diabatic heating, and stationary nonlinearity, for Feb. Contour interval for (a) is 10 m, and for (b) and (c) 5 m.

experiments are also conducted for January. The eddy vorticity forcing also plays a dominant role in maintaining the January response. Unlike the February case, the transient eddies in January force an anomalous ridge northeast of the Gulf of Alaska (not shown).

Having established that the different responses in the GCM are primarily associated with differences in the eddy forcing at equilibrium, the following question arises: what has caused the anomalous flows and the transients to be different in the first place? The only external forcing directly imposed in the GCM experiments is the SST anomaly, identical in January and February. The anomalous heating induced by the SST anomaly is also essentially similar in the two months. Does a similar heating excite different anomalous flows in January and February? Or, are the eddy feedbacks on the heating-induced anomalous flows substantially different in the two months, leading to different equilibrium responses? These issues are investigated in the following two sections.

4. The role of diabatic heating

We examine in this section how the atmosphere responds to a midlatitude heating in a linear model without eddy feedback and how such a response may be affected by the heating structure and the background flow. The diabatic heating from the GCM runs depicted in Fig. 3 shows that at equilibrium the heating is very weak because the atmosphere has adjusted to the imposed SST anomaly. Initially, however, the heating should be much stronger when the surface heat fluxes are stronger. The surface heat fluxes are proportional to the air–sea temperature difference. Initially, the anomalous air–sea temperature difference equals the SST anomaly, with a maximum near 2.5 K. At equilibrium, the temperature difference between the ocean and the air near the surface is about seven times weaker. Thus, the initial anomalous heating is estimated to be roughly seven times stronger than that at equilibrium. The heating pattern is assumed to resemble the positive center in Fig. 3a without the surrounding features. The initial heating thus defined is shown in Fig. 7a with a maximum depth-averaged heating rate of 2.5 K day^{-1}. The heating is further assumed to decay monotonically upward with an idealized profile, σ^n, where $\sigma = p/p_0$ ($p_0 = 1000$ mb), and n determines the decay rate. Larger n defines a shallower heating and vice versa. The equilibrium heating distri-

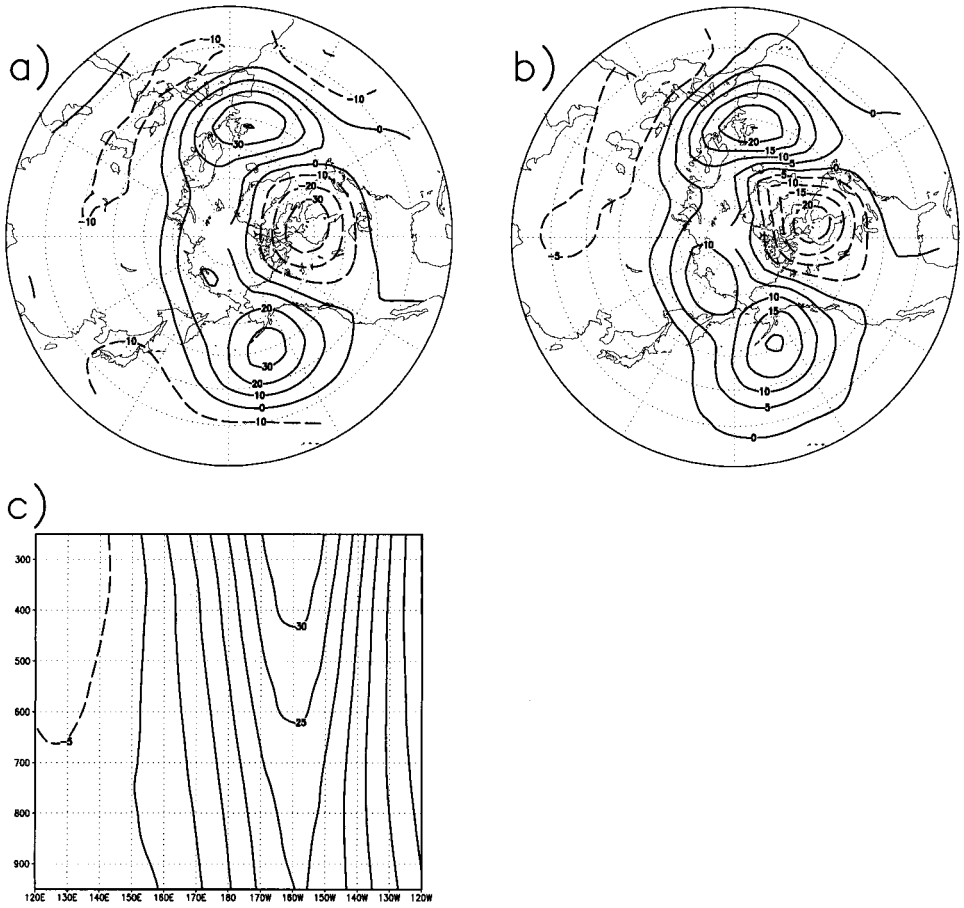

FIG. 6. Same as Fig. 5 but for the response to the eddy vorticity forcing only.

butions in the GCM approximately match the profile of $n = 4$. In the initial stages, the heating should be shallower with profiles of greater n. The vertical profile for $n = 8$ is shown in Fig. 7b.

The LBM response to the idealized initial heating defined in Fig. 7 for the February basic state is shown in Fig. 8. The anomalous flow directly induced by the heating is largely confined to the Pacific sector. The anomalous height is characterized by a downstream ridge in the upper troposphere (Fig. 8a) and a trough below, over the heating (Fig. 8b). The vertical distributions of the height anomalies are shown in Fig. 8c for a cross section dissecting the ridge maximum along 45°N. The height response to the heating is baroclinic with a trough extending beyond 800 mb. The vertical extension of the trough is determined by the vertical profile of the heating (Hoskins and Karoly 1981; Hendon and Hartmann 1982). The more the heating is confined to the surface the shallower the trough is. We have examined the LBM response to the heating with various vertical profiles. For the profile of $n = 20$, the trough is very shallow and confined below 850 mb, and the downstream ridge becomes nearly equivalent barotropic. For the profiles varying between $n = 8$ and $n = 20$ the upper-level response over the Pacific is not greatly different from that shown in Fig. 8a, resembling the ridge produced by the GCM (Fig. 2b). Downstream of the Pacific, the direct response to the heating is very weak.

The LBM response to the heating defined in Fig. 7 for the January basic state is shown in Fig. 9. The anomalous flow induced by the heating in January is similar to that in February in terms of both the vertical and horizontal structures. A closer comparison suggests that the upper-level ridge in January is centered slightly northeast of that in February. Nevertheless, the difference between the LBM responses in the two months is far less drastic than that in the GCM. Experiments with different heating profiles are also conducted for January. The results are similar to those for February described above. The GCM data reveal that the anomalous heating distributions at equilibrium in January and February are not greatly different over the SST anomaly, even though the different anomalous circulations have resulted in different downstream cooling. Thus, there is no reason to suggest that the initial anomalous heating should be different in the two months. The different GCM responses, therefore, are not attributable to the anomalous

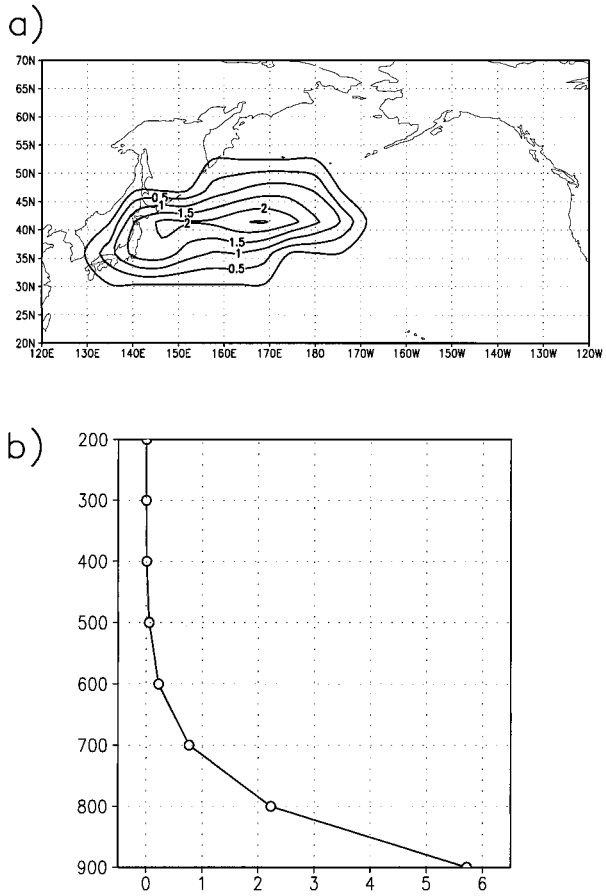

FIG. 7. (a) Idealized initial heating pattern with depth-averaged heating rates, and (b) the vertical heating distributions defined by σ^8. Contour interval for (a) is 0.5 K day^{-1}.

flows directly induced by the heating in the absence of eddy feedbacks. Do the transient eddies exert different feedback on the heating-induced anomalous flows in January and February? This question is addressed below in section 5.

5. The role of eddy feedback

The feedback of transient eddies on the heating-induced anomalous flows in January and February is examined by conducting experiments with the STM. As described above, the STM is a linear model designed to approximate the synoptic-scale transient eddy statistics associated with a given mean flow. The STM experiments are first performed with the unperturbed GCM background flows of January and February, respectively. The climatological synoptic eddy streamfunction variance and the streamfunction tendency due to the eddy vorticity fluxes produced by the STM for the two months are shown in Figs. 10a–d for 300 mb. The storm tracks are stronger and centered farther downstream in January than in February over both oceans, and particularly so over the Atlantic. The Pacific storm tracks in January appear to have a more tilted exit toward the northeast, indicated by the higher variance east of the Gulf of Alaska (Fig. 10a). These differences are consistent with the background flow differences depicted in PRH (their Figs. 2 and 15).

To verify that the eddy statistics produced by the STM are representative of the GCM synoptic transients, the climatological synoptic eddy statistics are calculated using the GCM daily data. Daily GCM data are accumulated from a 108-month control run for perpetual January. A 61-point 1–8-day bandpass filter is applied to isolate the synoptic eddy component. The GCM eddy statistics shown in Figs. 10e,f agree favorably with those simulated by the STM for January, indicating that it is reasonable to use the STM to diagnose the sensitivity of the GCM synoptic eddy statistics to large-scale flow perturbations.

We next run the STM with the heating-induced anomalous flows shown in Figs. 9 and 8 added to the January and February basic states, respectively. The anomalous eddy vorticity forcing is then obtained by subtracting the streamfunction tendency of the control run from that of the anomaly run. The eddy forcing in turn is used to drive the LBM. By comparing the anomalous flows driven by the heating and by the transients the nature of the eddy feedbacks is diagnosed. The framework of the experiments performed in sections 4 and 5 is summarized schematically as follows:

(a) $Q' \rightarrow$ LBM
$\rightarrow \Psi_1'$ (heating-induced anomalous flow),

(b) $\Psi_1' \rightarrow$ STM $\rightarrow \Psi_t'$ (anomalous eddy forcing),

(c) $\Psi_t' \rightarrow$ LBM
$\rightarrow \Psi_2'$ (eddy-driven anomalous flow),

where Q' represents the idealized anomalous heating. The following discussion will focus mainly on the Pacific sector as the STM is found to be overly sensitive to the background flow changes over the Atlantic. Causes for this sensitivity remain to be investigated and are beyond the scope of this study. To avoid this problem, only the eddy forcing over the Pacific half of the domain (90°–270°E, 0°–90°N) is used to drive the LBM.

The heating-induced anomalous flows at 250 mb in January and February are redrawn in Figs. 11a,b. Again, the height responses look similar in the two months except the ridge in January is centered slightly to the northeast. The corresponding anomalous eddy streamfunction variance produced by the STM is shown in Figs. 11c,d. The variance distributions over the Pacific suggest different eddy reorganizations in the two months. In January, the anomalous variance represents a weakening of the climatological storm tracks, while in February the anomalous variance represents a northward deflection of the storm tracks. The anomalous streamfunction tendency due to the eddy vorticity fluxes

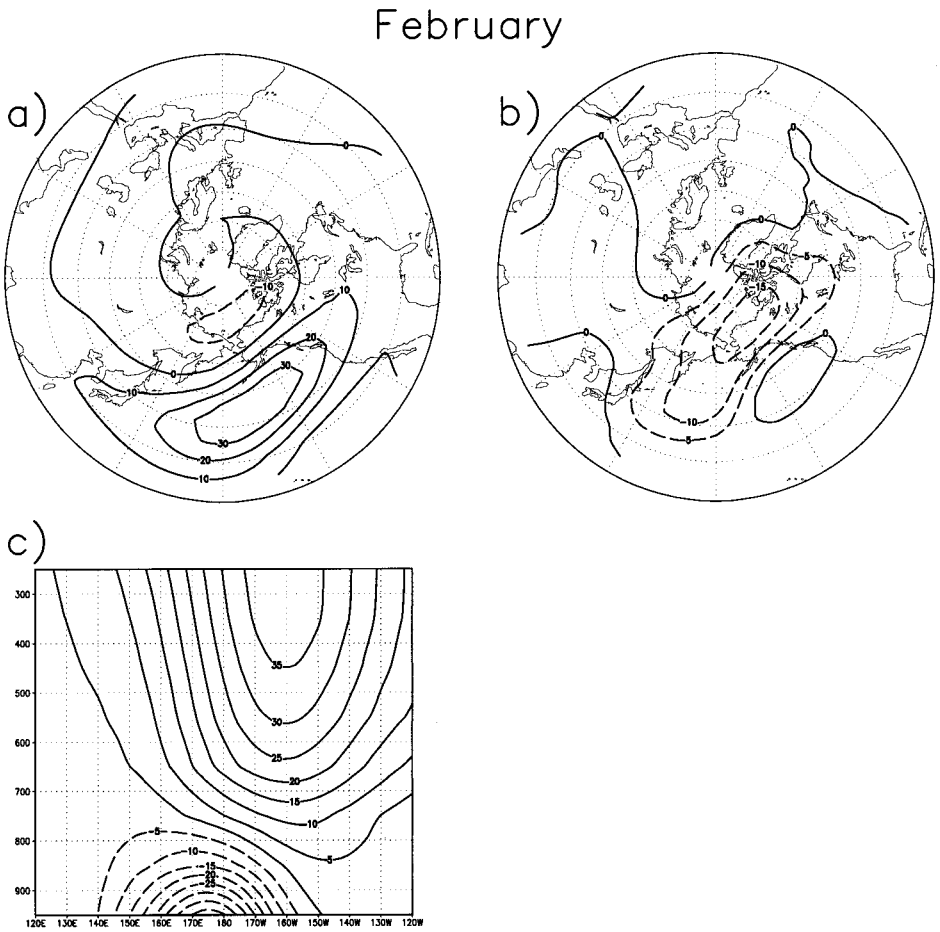

FIG. 8. The LBM geopotential height response at (a) 250 mb, (b) 850 mb, and (c) on a vertical cross section along 45°N, to the idealized heating for Feb. Contour interval for (a) is 10 m, and for (b) and (c) 5 m.

is shown in Figs. 11e,f. The transient eddies provide a positive tendency center in both months, but in January the eddy forcing is stronger and centered over the Gulf of Alaska. In February the forcing is centered at the date line near 40°N, slightly upstream of the heating-induced anomalous ridge.

The LBM responses to the eddy forcing of the Pacific domain are shown in Figs. 11g,h. The differences between the eddy-driven anomalous flows are far greater than those directly induced by the heating. The anomalous height forced by the transients in January is almost in quadrature with that in February. The eddy forcing in January generates an anomalous ridge over the northeast of the Pacific extending into the polar region and a trough to the southwest. Thus, the transients in January act to shift the heating-induced anomalous ridge toward the northeast. By contrast, the eddy forcing in February generates an anomalous ridge almost in phase with that induced by the heating. The eddy-driven anomalous flows in both months have an equivalent barotropic structure. The STM experiments have also been performed with the anomalous flow induced by the heating of various vertical profiles. Varying the heating profiles between $n = 8$ and $n = 20$, the eddy feedbacks of January and February are found largely similar to those described above.

The STM results suggest that the GCM responses develop in the following manner. Initially, the anomalous heating from the SST anomaly is strong and confined mainly to the boundary layer. The heating excites an anomalous flow similar in January and in February with a trough near the surface and a ridge above, over the Pacific. The heating-induced anomalous flow then leads to changes in the storm tracks, producing anomalous eddy vorticity fluxes that are strongly dependent on the background flow. In January the eddy forcing acts to shift the heating-induced anomalous ridge toward the northeast, and in February it reinforces the ridge over the Pacific. Differences between the transient eddy feedbacks in the January and February cases eventually lead to different equilibrium balances. Meanwhile, the heating extends deeper and becomes weaker as the atmosphere adjusts to the SST anomaly, so that at equilibrium the anomalous eddy fluxes are the dominant

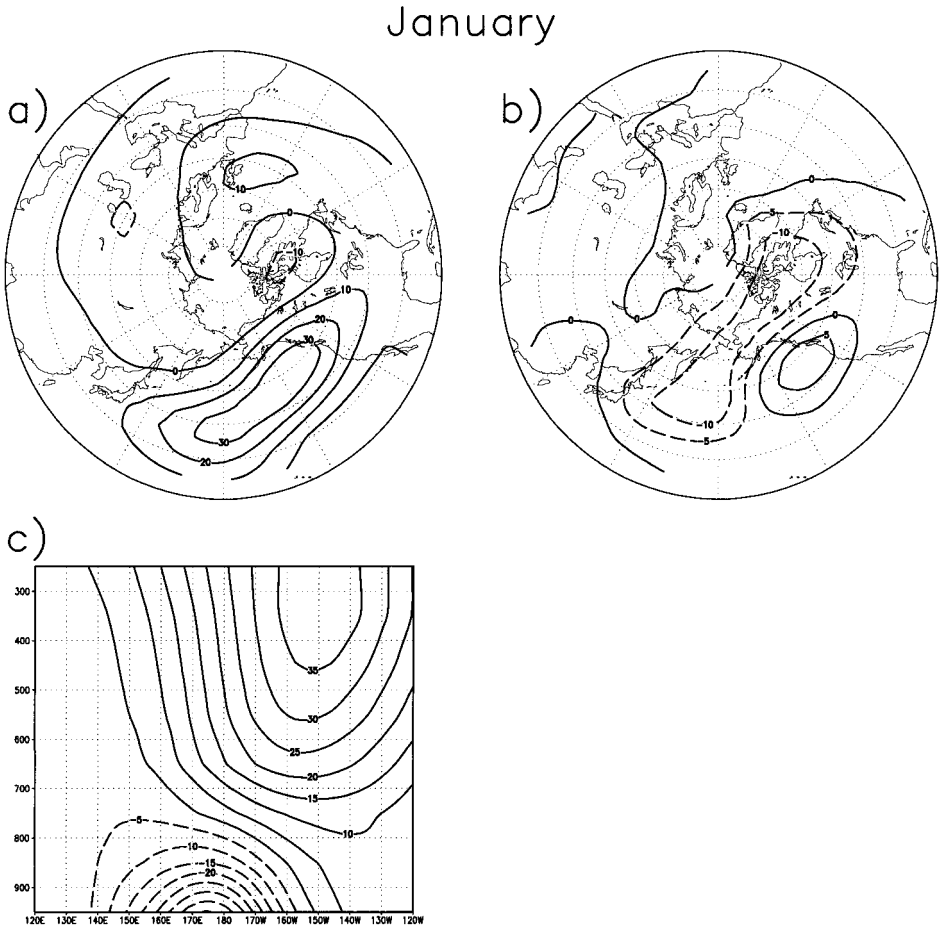

FIG. 9. Same as Fig. 8 but for January.

forcing mechanism. The eddy-driven anomalous flow has an equivalent barotropic structure. Thus, the response to the SST anomaly evolves from an initial baroclinic response to the heating to an equilibrium response with a nearly equivalent barotropic structure. This picture is particularly clear in the February case as the eddy feedback reinforces the heating-induced ridge in place. The January case is more complicated as the eddy-driven anomalous flow is not in phase with the heating-induced response. To actually reach the equilibrium balances, one could presumably continue to iterate the results between the LBM and the STM. We do not do so as the linear models are only approximate representations of the real atmosphere. More iterations will inevitably incorporate more errors into the results. The above experiments are intended to illustrate the differences between the eddy feedback in the two months and elucidate their role in causing the GCM equilibrium solutions to diverge.

We next address the question of how well the GCM responses represent the behavior of the real atmosphere by conducting the idealized model experiments with the observed winter background flow. To make the experiments general and independent of the GCM data, an elliptic heating pattern with a maximum depth-averaged heating rate of 2.5 K day^{-1} is used (Fig. 12). The vertical heating profile is set to be the same as that shown in Fig. 7b. The basic state is the observed December–February flow for the period of 1973–95. The climatological eddy statistics produced by the STM for the observed winter state are shown in Fig. 13 for 300 mb. Both the eddy streamfunction variance and the streamfunction tendency due to the vorticity fluxes are largely in good agreement with those calculated from observations by WS (see their Figs. 1 and 3).

The LBM height response to the elliptic heating centered at 40°N and 160°E is shown in Fig. 14a for 250 mb. In comparison with the height responses in GCM January and February (Figs. 11a,b), the ridge over the Pacific is less zonally elongated with a wave train spreading downstream. This difference is due to the background flow, and not the shape of the heating, since the LBM produces a similar response using the heating distribution shown in Fig. 7a. The height response over the Pacific has a baroclinic structure with a trough in

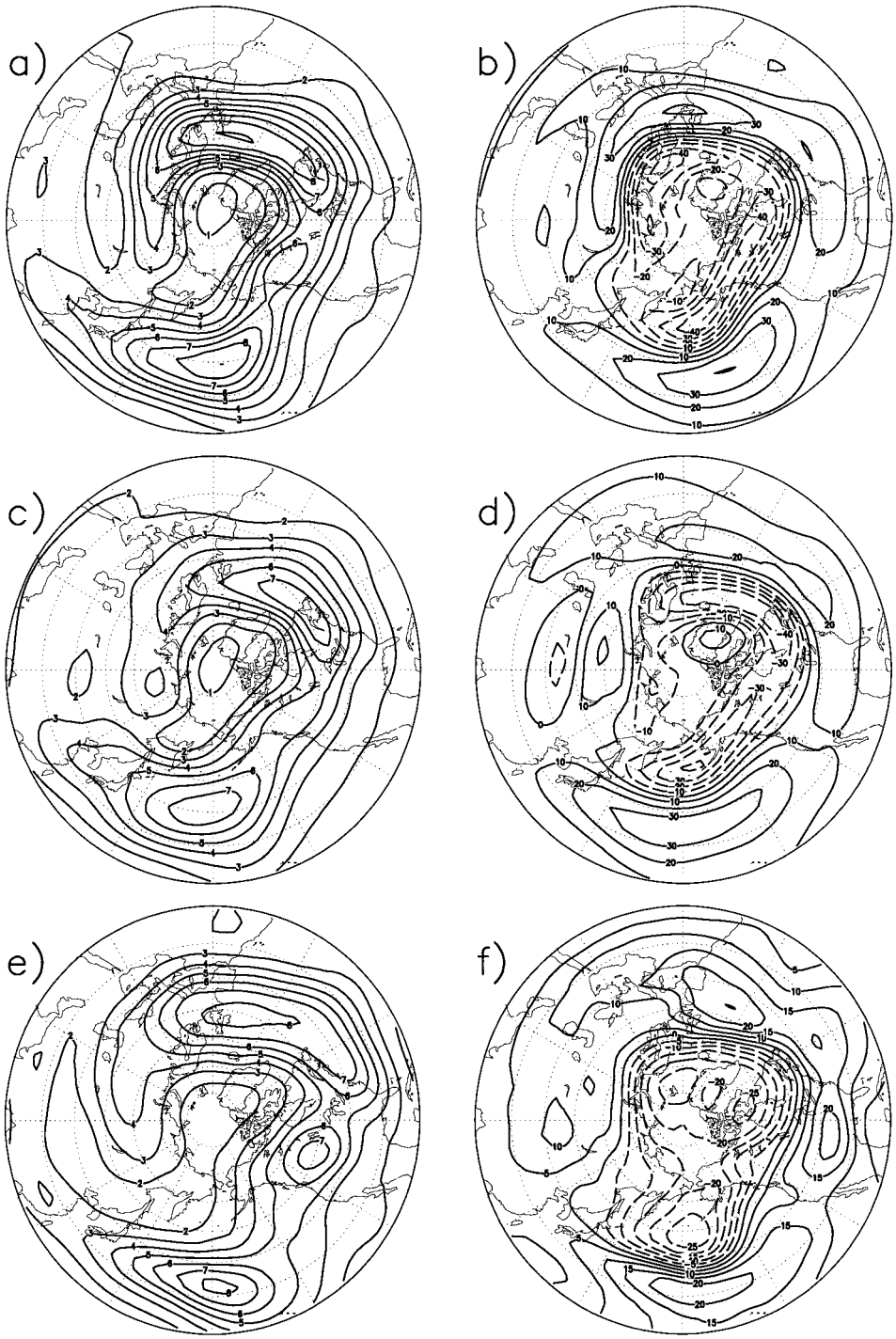

FIG. 10. The 300-mb eddy streamfunction variance and the streamfunction tendency due to eddy vorticity fluxes produced by the STM (a) and (b) for Jan and (c) and (d) for Feb, and those produced by the GCM (e) and (f) for Jan. Contour interval for (a), (c), and (e) is 1×10^{13} m^4 s^{-2}, for (b) and (d) 10 m^2 s^{-2}, and for (f) 5 m^2 s^{-2}.

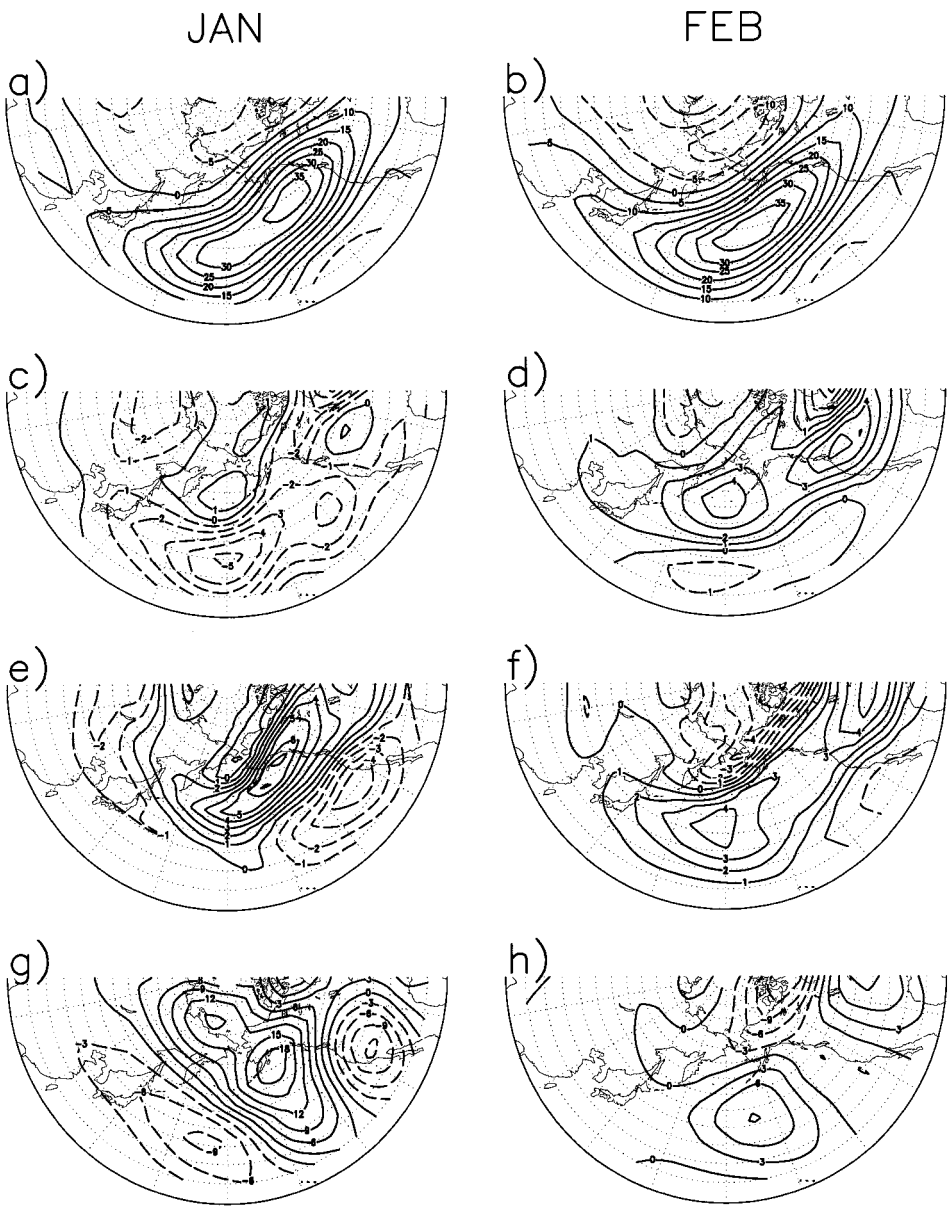

FIG. 11. (a) The LBM geopotential height response to the idealized heating for Jan at 250 mb, and (c) the corresponding anomalous eddy streamfunction variance, (e) anomalous streamfunction tendency due to eddy vorticity fluxes produced by the STM, and (g) the LBM height response to the eddy vorticity forcing. The right panels (b), (d), (f), and (h) are the same as the left but for Feb. Contour interval for (a) and (b) is 5 m, for (c) and (d) 1×10^{12} m^4 s^{-2}, for (e) and (f) 1 m^2 s^{-2}, and for (g) and (h) 3 m.

the lower troposphere, similar to that in GCM January and February.

With the heating-induced anomalous flow added to the observed basic state, the STM produces the anomalous eddy streamfunction variance shown in Fig. 14c. The anomalous variance over the Pacific is dominated by a positive center north of the storm tracks, again indicating a northward shift of the storm track. The anomalous streamfunction tendency due to the eddy vorticity fluxes is shown in Fig. 14e. There is a positive tendency center over the Pacific, slightly upstream of the heating-induced anomalous ridge. The eddy forcing in observed winter bears a stronger resemblance to that in GCM February than January. The LBM height response to the eddy forcing is shown in Fig. 14g. The eddy forcing produces an anomalous ridge over the Pacific, in phase with that induced by the heating. The eddy feedbacks thus reinforce the heating-induced anomalous ridge, similar to what occurred for GCM February. The observed winter flow, however, exhibits

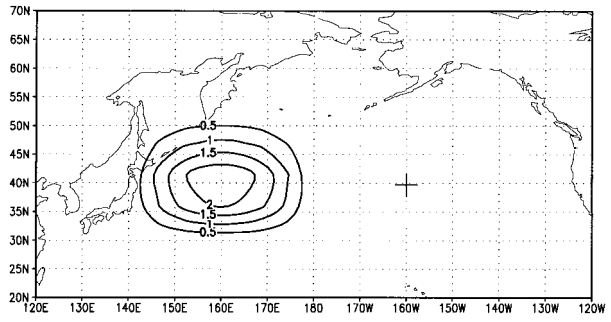

FIG. 12. Idealized elliptical heating pattern centered at 40°N and 160°E with depth-averaged heating rates. Contour interval is 0.5 K day^{-1}. Another heating position of 40°N and 160°W is marked by a cross.

a stronger sensitivity to the eddy forcing, resulting in a ridge nearly twice as strong as that in GCM February. This suggests that in nature the atmospheric response to an SST anomaly over the western Pacific is likely similar to the February GCM response but stronger.

The above results further demonstrate that the nature of eddy feedback on the heating-induced anomalous flow can be affected by the characteristics of the background flow. As suggested by Ting and Peng (1995) this sensitivity to the background flow may be related to the changes of the heating position relative to the storm tracks. If so, by varying the heating position relative to a given background flow one may also find significant changes in eddy feedback. To validate this hypothesis the idealized model experiments with observed winter mean flow are repeated with the heating shifted to 40°N and 160°W, and the corresponding results are shown in Figs. 14b, 14d, 14f, and 14h. With the heating-induced anomalous ridge shifted 40° downstream, the transient eddies reorganize by extending the storm tracks farther northeast. The anomalous flow driven by the eddy forcing (Fig. 14h) is nearly in quadrature with that induced by the heating (Fig. 14b). The eddy feedback no longer reinforces the heating-induced anomalous ridge. Thus, it is unlikely that the real atmosphere can produce an equivalent barotropic ridge response to warm SST anomalies over the eastern Pacific.

Other experiments with the heating in different locations have been performed. The reinforcement of the anomalous ridge by the transients is found to be the strongest with the heating centered at 40°N and 170°E. These results demonstrate that the nature of eddy feedback indeed depends crucially on the heating position relative to the storm tracks. In nature, warm SST anomalies over the western Pacific are likely more effective in exciting and maintaining an equivalent barotropic ridge.

6. Summary and discussion

The GCM experiments of PRH showed that the atmospheric response to a midlatitude warm SST anomaly over the Pacific is sensitive to the background flow. In January the model produces an anomalous trough decaying with height, whereas in February, a nearly equivalent barotropic ridge growing with height. In order to understand the development and maintenance of the GCM responses, and especially the physical mechanisms leading to their differences, a series of experiments with idealized models are conduced.

Two idealized models are used: a linear baroclinic model and a linear storm track model. The LBM is first used to determine the maintenance of the GCM responses. The results show that the GCM equilibrium responses are predominantly maintained by the eddy vorticity fluxes. The diabatic heating at equilibrium is very weak and contributes little to the equilibrium bal-

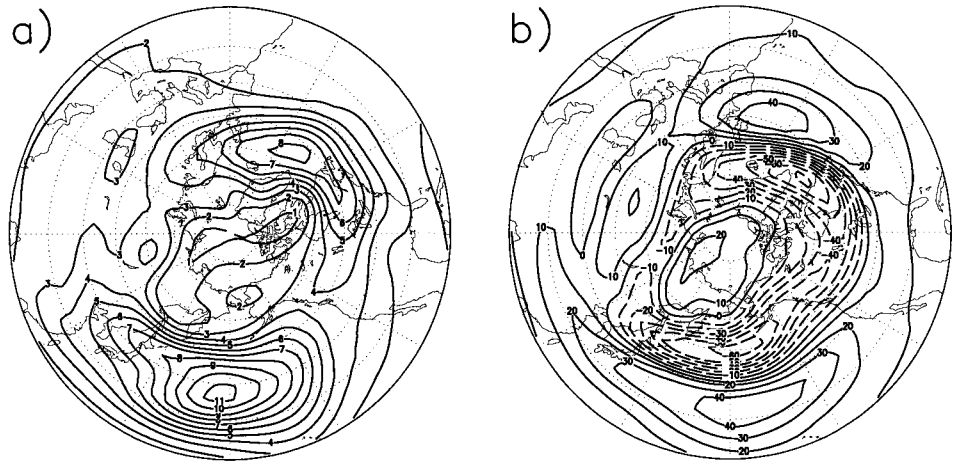

FIG. 13. (a) The 300-mb eddy streamfunction variance and (b) the streamfunction tendency due to eddy vorticity fluxes, produced by the STM for observed winter. Contour interval for (a) is 1×10^{13} m^4 s^{-2}, and for (b) 10 m^2 s^{-2}.

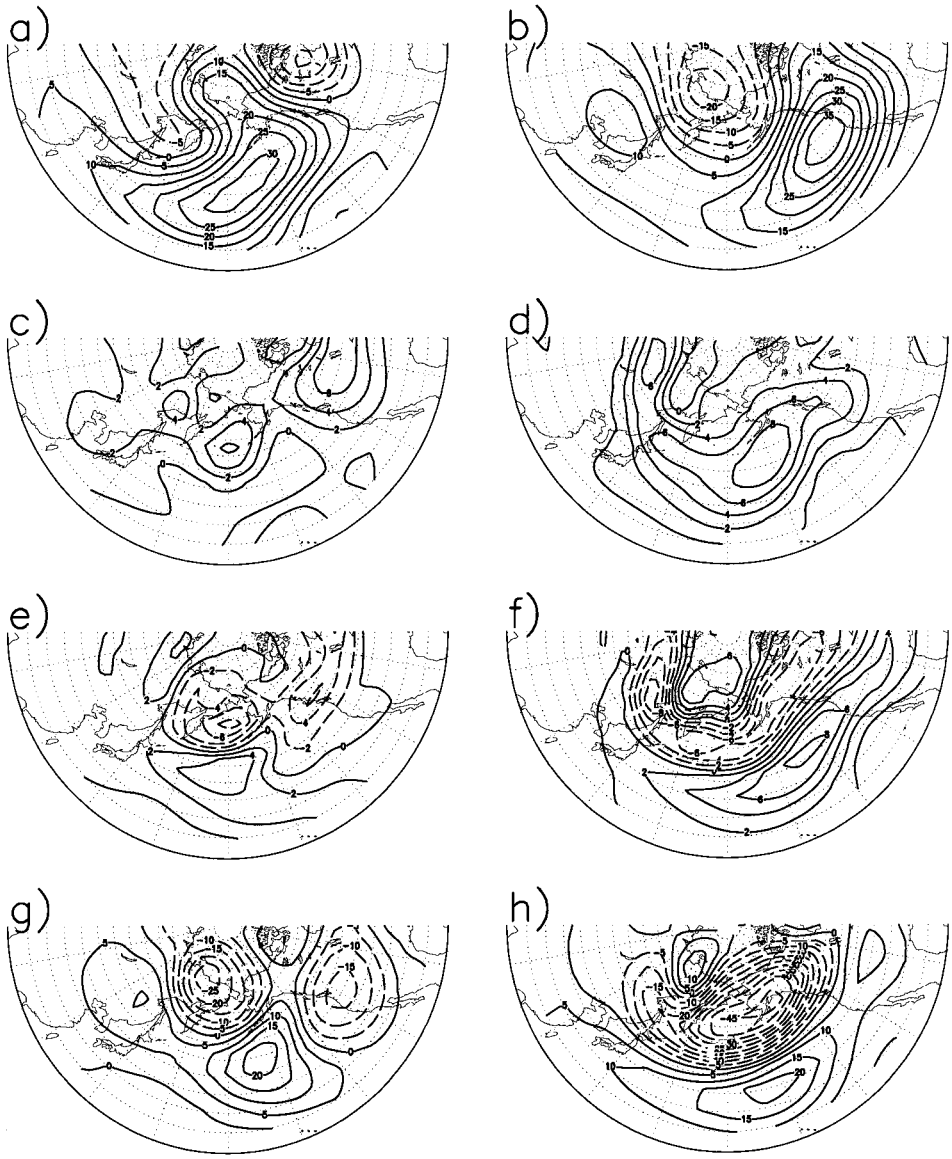

FIG. 14. (a) The LBM geopotential height response to the elliptical heating centered at 40°N and 160°E for observed winter at 250 mb,(c) the corresponding anomalous eddy streamfunction variance and (e) anomalous streamfunction tendency due to eddy vorticity fluxes produced by the STM, and (g) the LBM height response to the eddy vorticity forcing. The right panels (b), (d), (f), and (h) are the same as the left but for the heating centered at 40°N and 160°W. Contour interval for (a), (b), (g), and (h) is 5 m, for (c) and (d) 2 $\times$ 10^{12} m^4 s^{-2}, and for (e) and (f) 2 m^2 s^{-2}.

ances. However, the anomalous heating initially induced by the SST anomaly is estimated to be much stronger. The LBM is used to examine the atmospheric response to an idealized initial heating, in the absence of eddy feedbacks, and its dependence on the heating structure and the background flow. Without eddy feedback the model response to the idealized heating is similar in January and February. The anomalous flow directly induced by the heating is baroclinic with a trough in the lower troposphere and a ridge above. The vertical extent of the trough is determined by the vertical distributions of the heating.

Eddy feedback on the heating-induced anomalous flow is examined using the STM. The anomalous eddy statistics produced by the STM in January and February are very different. The eddy forcing in January acts to shift the heating-induced upper-level ridge toward the northeast of the Gulf of Alaska, whereas in February it acts to reinforce the ridge over the Pacific. The idealized model results are in good agreement with the equilib-

rium responses produced by the GCM, where an equivalent barotropic ridge is found over the Pacific in February but shifted to the northeast of the Gulf of Alaska in January. This suggests that differences in the eddy feedbacks on the initially similar heating-induced anomalous flows initiate the chain of events leading to the very different January and February GCM equlibrium solutions.

Idealized model experiments are also conducted with the observed winter mean flow. The transients are found to reinforce the heating-induced anomalous ridge over the Pacific, similar to that in GCM February. With observed background flow, however, the eddy forcing generates an anomalous flow nearly twice as strong as that in GCM February. These results suggest that the real atmosphere likely responds to warm SST anomalies over the western Pacific with an equivalent barotropic ridge, similar to that in GCM February, but more strongly. Similar experiments are also performed with the idealized heating moved to other locations. With the heating shifted 40° downstream the eddy-driven anomalous flow no longer reinforces the anomalous ridge induced by the heating. Thus, the nature of eddy feedback depends strongly on the heating position relative to the storm tracks.

The idealized model experiments with the observed flow provide insights into the possible impact of midlatitude SST anomalies in nature. Our results suggest that midlatitude atmosphere–ocean interactions are location dependent. Warm SST anomalies over the western Pacific are likely more effective in initiating a positive eddy feedback leading to a strong anomalous ridge with an equivalent barotropic structure. As mentioned earlier, such a ridge response has the potential to reinforce the SST anomaly (Latif and Barnett 1994; Peng et al. 1995). The resulting positive atmosphere–ocean feedback can lead to persistent blocks over the central Pacific, influencing not only seasonal-to-interannual variability but also decadal climate variability through their integrated effects (Latif and Barnett 1994; Deser et al. 1996; Nakamura et al. 1997a; Nakamura et al. 1997b). SST anomalies over the eastern Pacific perhaps play a more passive role in the coupled system (Alexander 1990; Lau and Nath 1996), since the associated heating-induced anomalous flow is not likely to initiate an effective eddy feedback.

A realistic evaluation of the impact of midlatitude SST anomalies on the atmosphere requires a GCM with good representations of observed climatology. This study illustrates how errors in model climatologies, particularly in the vicinity of the storm tracks, can lead to unrealistic simulations of the atmospheric response to midlatitude SST anomalies. The unsatisfactory behavior of the transient eddies in the GCM is perhaps related to a tilted Pacific jet. In reality, the jet is zonally oriented during the winter months. Further investigation is needed to ascertain the nature and causes of these model errors. Given the crucial role played by the transients in modulating and maintaining the GCM response to SST anomalies, further study is also needed to elucidate the mechanisms by which the background flow affects the eddy feedbacks. An improved representation of transient eddy feedbacks in GCMs is clearly essential to a better understanding of the role of midlatitude oceans in climate variability.

Acknowledgments. Shiling Peng gratefully acknowledges the valuable input of Drs. Grant Branstator and Walter A. Robinson by generously sharing their knowledge on the subject. Their support and encouragement during the course of this study are greatly appreciated. Dr. Robinson also provided helpful comments and suggestions on the draft of this paper. It is a pleasure to thank the reviewers, Drs. Tim N. Palmer and Hisashi Nakamura, for their thoughtful and encouraging comments. We also thank Dr. Joseph J. Barsugli for sharing the scripts of accumulating eddy fluxes and diabatic heating from the GCM runs. This work is funded in part by Grant GC97-244 from the NOAA Climate and Global Change Program.

REFERENCES

Alexander, M. A., 1990: Simulation of the response of the North Pacific Ocean to the anomalous atmospheric circulation associated with El Nino. *Climate Dyn.,* **5,** 53–65.

Branstator, G., 1992: The maintenance of low-frequency atmospheric anomalies. *J. Atmos. Sci.,* **49,** 1924–1945.

——, 1995: Organization of storm track anomalies by recurring low-frequency circulation anomalies. *J. Atmos. Sci.,* **52,** 207–226.

Deser, C., and M. L. Blackmon, 1995: On the relationship between tropical and North Pacific sea surface temperature variations. *J. Climate,* **8,** 1677–1680.

——, and M. S. Timlin, 1997: Atmosphere–ocean interaction on weekly timescales in the North Atlantic and Pacific. *J. Climate,* **10,** 393–408.

——, M. A. Alexander, and M. S. Timlin, 1996: Upper-ocean thermal variations in the North Pacific during 1970–1991. *J. Climate,* **9,** 1840–1855.

Ferranti, L., F. Molteni, and T. N. Palmer, 1994: Impact of localized tropical and extratropical SST anomalies in ensembles of seasonal GCM integrations. *Quart. J. Roy. Meteor. Soc.,* **120,** 1613–1645.

Hendon, H. H., and D. L. Hartmann, 1982: Stationary waves on a sphere: Sensitivity to thermal feedback. *J. Atmos. Sci.,* **39,** 1906–1920.

Hoskins, B. J., and D. Karoly, 1981: The steady linear response of a spherical atmosphere to thermal and orographic forcing. *J. Atmos. Sci.,* **38,** 1179–1196.

Kushnir, Y., and N.-C. Lau, 1992: The general circulation model response to a North Pacific SST anomaly: Dependence on time scale and pattern polarity. *J. Climate,* **5,** 271–283.

——, and I. M. Held, 1996: Equilibrium atmospheric response to North Atlantic SST anomalies. *J. Climate,* **9,** 1208–1220.

Latif, M., and T. P. Barnett, 1994: Causes of decadal climate variability over the North Pacific and North America. *Science,* **266,** 634–637.

Lau, N.-C., and M. J. Nath, 1994: A modeling study of the relative roles of tropical and extratropical SST anomalies in the variability of the global atmosphere–ocean system. *J. Climate,* **7,** 1184–1207.

——, and ——, 1996: The role of the ''atmospheric bridge'' in linking

tropical Pacific ENSO events to extratropical SST anomalies. *J. Climate,* **9,** 2036–2057.

Nakamura, H., G. Lin, and T. Yamagata, 1997a: Decadal climate variability in the North Pacific during the recent decades. *Bull. Amer. Meteor. Soc.,* **78,** 2215–2225.

——, M. Nakamura, and J. L. Anderson, 1997b: The role of high- and low-frequency dynamics in blocking formation. *Mon. Wea. Rev.,* **125,** 2074–2093.

Palmer, T. N., and Z. Sun, 1985: A modelling and observational study of the relationship between sea surface temperature in the northwest Atlantic and atmospheric general circulation. *Quart. J. Roy. Meteor. Soc.,* **111,** 947–975.

Peng, S., and J. Fyfe, 1996: The coupled patterns between sea level pressure and sea surface temperature in the midlatitude North Atlantic. *J. Climate,* **9,** 1824–1839.

——, L. A. Mysak, H. Ritchie, J. Derome, and B. Dugas, 1995: The differences between early and midwinter atmospheric responses to sea surface temperature anomalies in the northwest Atlantic. *J. Climate,* **8,** 137–157.

——, W. A. Robinson, and M. P. Hoerling, 1997: The modeled atmospheric response to midlatitude SST anomalies and its dependence on background circulation states. *J. Climate,* **10,** 971–987.

Pitcher, E. J., M. L. Blackmon, G. T. Bates, and S. Munoz, 1988: The effect of North Pacific sea surface temperature anomalies on the January climate of a general circulation model. *J. Atmos. Sci.,* **45,** 173–188.

Ting, M., 1991: The stationary wave response to a midlatitude SST anomaly in an idealized GCM. *J. Atmos. Sci.,* **48,** 1249–1275.

——, and N.-C. Lau, 1993: A diagnostic and modeling study of the monthly mean wintertime anomalies appearing in a 100-year GCM experiment. *J. Atmos. Sci.,* **50,** 2845–2867.

——, and S. Peng, 1995: Dynamics of the early and middle winter atmospheric responses to the northwest Atlantic SST anomalies. *J. Climate,* **8,** 2239–2254.

Wallace, J. M., and Q. Jiang, 1987: On the observed structure of the interannual variability of the atmosphere/ocean climate system. *Atmospheric and Ocean Variability,* H. Cattle, Ed., Royal Meteorological Society, 17–43.

Whitaker, J. S., and P. D. Sardeshmukh, 1998: A linear theory of extratropical synoptic eddy statistics. *J. Atmos. Sci.,* **55,** 237–258.